Bioinformatic analysis of PD 1 checkpoint blockade responsive immune microenvironment in severe influenza infection

huilin ou
Ningbo lihuili Hospital https://orcid.org/0000-0002-4265-2811
Keda Chen
shulan
Hongcheng Wu
ningbo lihuili hospital
hangping Yao (yaohangping@zju.edu.cn)
First Hospital of Zhejiang Province: Zhejiang University School of Medicine First Affiliated Hospital

Research

Keywords: PD 1/PD L1, influenza, immune checkpoint, immune microenvironment

Posted Date: October 18th, 2021

DOI: https://doi.org/10.21203/rs.3.rs-962677/v1

Bioinformatic analysis of PD-1 checkpoint blockade–responsive immune microenvironment in severe influenza infection

Huilin Ou[1], Keda Chen[2], Hongcheng Wu[1], Hangping Yao[3*],

1 Ningbo Medical Centre, Li Huili Hospital affiliated of Ningbo University, Ningbo 315040, China

2 Shulan International Medical College, Zhejiang Shuren University, Hangzhou 310015, China

3 State Key Laboratory for Diagnosis and Treatment of Infectious Diseases, First Affiliated Hospital, Zhejiang University School of Medicine, Hangzhou 310003, China

*Corresponding author: Hangping Yao

Address: First Affiliated Hospital, Zhejiang University School of Medicine, Hangzhou, China

Tel: 86-574-87236580, Fax: 86-574-87236582, Email: *yaohangping@zju.edu.cn*

Key words: PD-1/PD-L1, influenza, KEGG, Gene

Abstract：

Background: The programmed cell death 1 (PD-1)/PD-1 ligand 1 (PD-L1) signaling pathway is significantly upregulated in severe influenza virus infection, which impairs the immune system and causes increased tissue inflammation and damage. Blocking this signaling pathway will reduce the damage, lower the virus titer in lung tissue, and alleviate the symptoms of infection to promote recovery. The aim of this study was to identify the key factors and regulatory mechanisms in the PD-1 checkpoint blockade–responsive immune microenvironment in severe influenza infection.

Methods: A BALB/c mouse model of severe influenza A/H1N1 infection was constructed, and whole-transcriptome sequencing of mice treated with PD-1 checkpoint blockade before severe

A/PR8(H1N1) influenza infection and IgG2a isotype control before infection were performed. Subsequently, the differential expression of nucleic acids between these two groups was analyzed, followed by functional interaction prediction analysis to investigate gene-regulatory circuits.

Results: In total, 84 differentially expressed (dif) mRNAs, 36 dif-microRNAs (miRNAs), 90 dif-lncRNAs (long noncoding RNAs), and 22 dif-circRNAs (circular RNAs) were found in PD-1 antagonist treated A/PR8(H1N1) influenza infection lung compared with the controls (IgG2a isotype control treated before infection). In spleens between the above two groups, 45 dif-mRNAs, 36 dif-miRNAs, 57 dif-lncRNAs, and 24 dif-circRNAs were identified. Direct function enrichment analysis of dif-mRNAs and dif-miRNAs showed that these genes were mainly involved in myocardial damage related to viral infection, mitogen activated protein kinase (MAPK) signaling pathways, RAP1 (Ras-related protein 1) signaling pathway, and Axon guidance. Finally, 595 interaction pairs were obtained for the lungs and 462 interaction pairs for the spleens were obtained in the competing endogenous RNA (ceRNA) complex network, in which the downregulated mmu-miR-7043-3p and Vps39-204 were enriched significantly.

Conclusions: The present study provided a basis for the identification of potential pathways and hub genes that might be involved in the PD-1 checkpoint blockade–responsive immune microenvironment in severe influenza infection.

Key words: PD-1/PD-L1, influenza, immune checkpoint, immune microenvironment

Background

Programmed cell death 1 (PD-1) is a negative immune checkpoint molecule that downregulates T cell activity after binding with its ligand, PD-1 ligand 1 (PD-L1), during immune

responses. In chronic infections or tumors, PD-1 overexpression after lasting antigen-exposure will impair the immune response to clear the pathogens or degenerate cells[1]. PD-1 blockade can restore T cell function, and is already used as a successful therapy in multiple cancer treatments[2-3]. The role of the PD-1/PD-L1 pathway in inhibiting immunity during chronic infections is well established[4]. Recently, its role in acute infections has aroused research attention[5]. The PD-1/PD-L1 pathway has been proven to not only dampen T cell responses and restrain memory T cells during some acute infections, but also limits the function of dendritic cells (DCs), macrophages, and T cell independent B cell responses. The precise mechanism by which the PD-1/PD-L1 pathway regulates immune responses during acute infection remains unclear.

Influenza virus, especially influenza A virus (IAV) infection, is a huge challenge to global public health, which, because of its high morbidity and mortality, and extremely high antigen mutation rate, has the possibility of causing epidemic outbreaks and even human-to-human transmission[6]. Severe infections often cause fatal pneumonia, which quickly leads to acute respiratory distress syndrome (ARDS) and multiple organ failure. In recent years, studies have proven that acute influenza virus infection, especially severe infections, induce upregulated expression of the PD-1/PD-L1 pathway in an interferon receptor signaling-dependent manner, which leads to degranulation dysfunction and exhaustion of immune cells, especially $CD8^+$ T cells[7].

The airway epithelium is the first barrier against influenza infection, which participates in host defense by producing cytokines and chemokines, and by regulating expression of surfactant proteins and adapter molecules. Experiments have confirmed that severe influenza virus infection can induce PD-1/PD-L1 signal overexpression and $PD\text{-}1^+$ cell migration to the lung, which plays

an important role in maintaining immune homeostasis[8-9]. The spleen is the largest secondary immune organ and combines the innate and adaptive immune systems, which are important for antibacterial and antifungal immune reactivity. The spleen is a highly organized lymphoid compartment that removes blood-borne microorganisms and cellular debris. PD-1 and PD-L1 expression are high in the spleen[10] and upregulation of PD-1 expression correlated well with reduced gamma interferon (IFN-γ) and tumor necrosis factor (TNF) production after virus inoculation.

The transcriptome reflects tissue activity at a given point in time, thus transcriptome expression studies provide an unbiased approach to investigate the PD-1 checkpoint blockade–responsive immune microenvironment during severe influenza infection. RNA sequencing (RNA-Seq) is a next-generation DNA sequencing method that determines the sequences of mRNAs[11], and has obvious advantages over microarray sequencing. RNA-seq identifies transcription initiation sites and new splicing variants, which makes it possible to precisely determine the exon and splicing isoform expression and to understand the complexity of eukaryotic transcriptomes comprehensively[12].

Methods

BALB/c mice (6 to 7 weeks old) were purchased from Joint Ventures SIPPER-BK Experimental Animal Co. (Shanghai, China). All animals were bred and maintained in specific pathogen-free conditions in accordance with the Care and Use of Laboratory Animals of Zhejiang Province and were approved by the local Ethics Committee. Six mice were divided into two groups: 1. The isotype control followed by A/PR8(H1N1) infection group (severe infection group, 50μL 10^6 median tissue culture infectious dose (TCID50) infective dose). 2. PD-1 antagonist followed with

A/PR8(H1N1) infection group. The PD-1 antagonist comprised an antibody against PD-1 (clone RMP1-14; BioXCell, Lebanon, NH, USA), which was administered via tail vein injection in 200 μg doses on days 1, 4, and 7 before infection. An antibody against IgG2a (clone 2A3; BioXCell) was used as the isotype control. Mice were chemically restrained with 2,2,2-tribromoethanol (avertin) before intranasal challenge with 50 μL of 10^6 TCID50 virus diluted in phosphate-buffered saline (PBS). Mice were sacrificed 6 days after virus inoculation and their lungs and spleens were collected.

Library preparation and sequencing for small RNAs

A total of 3 μg RNA per sample was used as input material, and sequencing libraries were generated using an NEB Next®Multiplex Small RNA Library Prep Set (NEB, Ipswich, MA, USA). Briefly, the NEB 3' SR Adaptor was ligated to the 3' end of microRNAs (miRNA), small interfering RNAs (siRNAs) and PIWI-interacting RNAs (piRNAs), then the SR RT Primer hybridized to the excess of 3' SR Adaptor and transformed the single-stranded DNA adaptor into a double-stranded DNA molecule. PCR amplification was performed, and then the amplicons were purified. DNA fragments corresponding to 140~160 bp were recovered and dissolved. Finally, library quality was assessed on an Agilent Bioanalyzer 2100 system (Agilent, Santa Clara, CA, USA) using DNA High Sensitivity Chips.

The clustering of samples was performed on a cBot Cluster Generation System using TruSeq SR Cluster Kit v3-cBot-HS (Illumina, San Diego, CA, USA). After cluster generation, the library preparations were sequenced on an Illumina Hiseq 2500/2000 platform and 50 bp single-end reads were generated.

Data analysis of small RNAs

Mapped small RNA tags were used to looking for known miRNAs. miRBase20.0 was used as the reference, and the modified software mirdeep2 and sRNA-tools-cli were used to obtain the potential miRNA and draw the secondary structures. The software miREvo and mirdeep2 were integrated to predict novel miRNAs. We followed the following priority rule: Known miRNA > rRNA > tRNA > snRNA > snoRNA > repeat > gene > NAT-siRNA > gene > novel miRNA > ta-siRNA to make every unique small RNA mapped to only one annotation. The known miRNAs used miFam.dat (http://www.mirbase.org/ftp.shtml) to look for families; novel miRNA precursors were submitted to Rfam (http://rfam.sanger.ac.uk/search/) to look for Rfam families. Predicting the target genes of the miRNAs was performed using miRanda. Differential expression analysis was performed using the DESeq R package (1.8.3) with a P-value of 0.05 set as the threshold. The P-values was adjusted using the Benjamini & Hochberg method.

Gene Ontology (GO) enrichment analysis was used on the target gene candidates of the differentially expressed miRNAs. We used KOBAS software to test the statistical enrichment of the target gene candidates in KEGG (Kyoto Encyclopedia of Genes and Genomes) pathways.

Library preparation and sequencing for lncRNAs

A total of 3 μg RNA per sample was used as input material to construct sequencing libraries, which were generated using the rRNA-depleted RNA by NEB Next® Ultra™ Directional RNA Library Prep Kit for Illumina®. The clustering of samples was performed on a cBot Cluster Generation System using TruSeq PE Cluster Kit v3-cBot-HS (Illumina), the libraries were sequenced on an Illumina Hiseq 4000 platform and 150 bp paired-end reads were generated.

Data analysis of lncRNAs

Clean data were obtained by removing reads containing adapter or poly-N sequences. An index of the reference genome was built using bowtie2 v2.2.8 and paired-end clean reads were aligned to the reference genome using HISAT2 v2.0.4. The mapped reads of each sample were assembled using StringTie (v1.3.1) in a reference-based approach. We used phyloFit to compute phylogenetic models for conserved and non-conserved regions and then submitted the model and HMM transition parameters to phyloP to compute a set of conservation scores of lncRNAs and coding genes. We clustered the genes from different samples using weighted gene co-expression network analysis (WGCNA) to search for common expression modules and then analyzed their function through functional enrichment analysis. Transcripts with P-adjust < 0.05 were assigned as differentially expressed. GO enrichment analysis and KEGG pathway enrichment analysis were performed as above.

Results

Differential Expression Analysis

In the differential expression analysis of lungs (Figure 1), 85 differentially expressed mRNAs (dif-mRNAs) were obtained, of which 76 were upregulated and 9 were downregulated; 36 differentially expressed miRNAs (dif-miRNAs) were identified, of which 19 were upregulated and 17 were downregulated; 90 differentially expressed lncRNAs (dif-lncRNAs) were obtained, including 70 upregulated and 20 downregulated; and 22 differentially expressed circRNAs (dif-circRNAs) were found, of which 13 were upregulated and 9 were downregulated.

In the spleen data, 45 dif-mRNAs were obtained, of which 18 were upregulated and 27 were

downregulated; 36 dif-miRNAs were identified, of which 19 were upregulated and 17 were downregulated; 57 dif-lncRNAs were obtained, including 22 upregulated and 35 downregulated; and 24 dif-circRNAs were found, of which 18 were upregulated and 6 were downregulated.

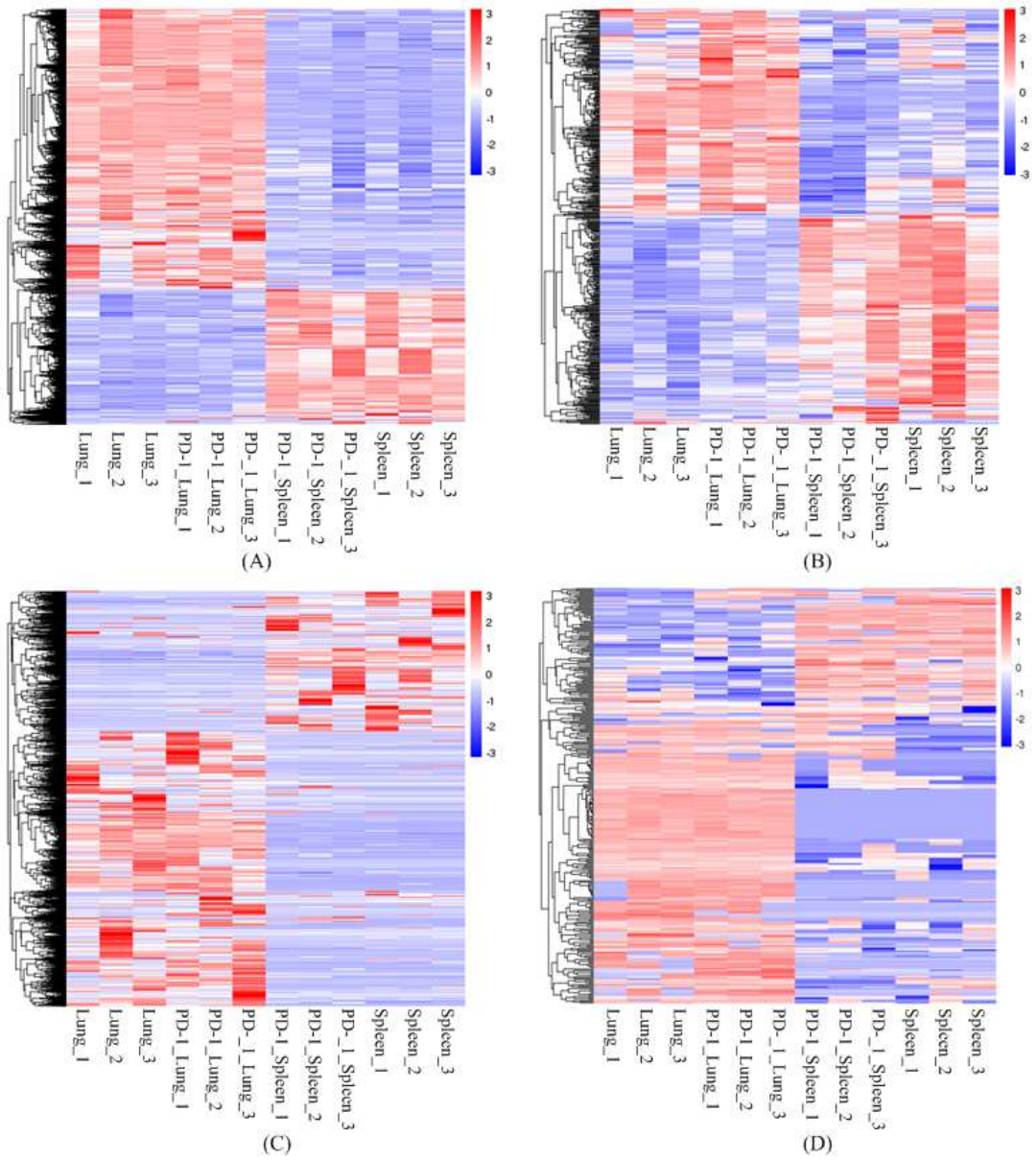

Figure 1. Heatmaps of differentially expressed nucleic acids. Heatmaps of differentially expressed mRNAs (A), differentially expressed miRNAs (B), differentially expressed lncRNAs (C), and differentially expressed circRNAs (D) of lungs and spleens of the following groups: PD-1 antagonist treatment followed by A/PR8(H1N1) infection group *vs*. isotype control followed by

160 A/PR8(H1N1) infection group. Red indicates upregulation, and blue indicates downregulation.

161 ***Functional enrichment analysis of dif-mRNAs and dif-miRNAs in lungs and spleens***

162 KEGG and GO analyses were used to investigate the functional associations of gene expression
163 changes. Targeted genes of dif-mRNA and dif-miRNAs of lungs and spleens of the two groups:
164 PD-1 antagonist followed with A/PR8(H1N1) infection group *vs.* Isotype control followed with
165 A/PR8(H1N1) infection were predicted (Figure 2 and Figure 3). The gene lists used in the
166 dif-mRNAs analysis contained 18455 and 17818 genes for lungs and spleens, respectively. 1290
167 and 1290 genes were analyzed for lungs and spleens for dif-miRNAs. For GO, biological process,
168 cellular component, and molecular function were selected as the annotation categories for
169 clustering. Once the tool identified enriched ontologies for a particular gene list, it clusters those
170 that have a statistically significant overlap in terms of their constituent genes. The dif-mRNAs
171 were enriched in 81 pathways in lungs and 36 pathways in spleens. dif-miRNAs were enriched in
172 274 pathways in lungs and 273 pathways in spleens. There was little degree of overlap of
173 dif-mRNAs and dif-miRNAs in lungs between the most enriched clusters. The most enriched
174 clusters of dif-mRNAs of lungs were related to muscle and heart biological behavior. More than
175 85% of the dif-miRNAs enriched clusters in lungs and spleens overlapped with each other,
176 including localization, metabolic process, positive regulation of metabolic process, and regulation
177 of molecular function in the biological process category; intracellular part, cytoplasm, intracellular,
178 and membrane-bounded organelle in the cellular component category; and protein binding,
179 enzyme binding, and molecular function regulator in the molecular function category.

180 Functional Enrichment analysis of mRNAs and miRNAs in lungs and spleens obtained from
181 severe IAV infection mice treated with anti-PD-1 antibody clearly highlighted myocardial damage

related to viral infection, mitogen-associated protein kinase (MAPK) signaling pathways, RAP1 (Ras-related protein 1) signaling pathway, and Axon guidance.

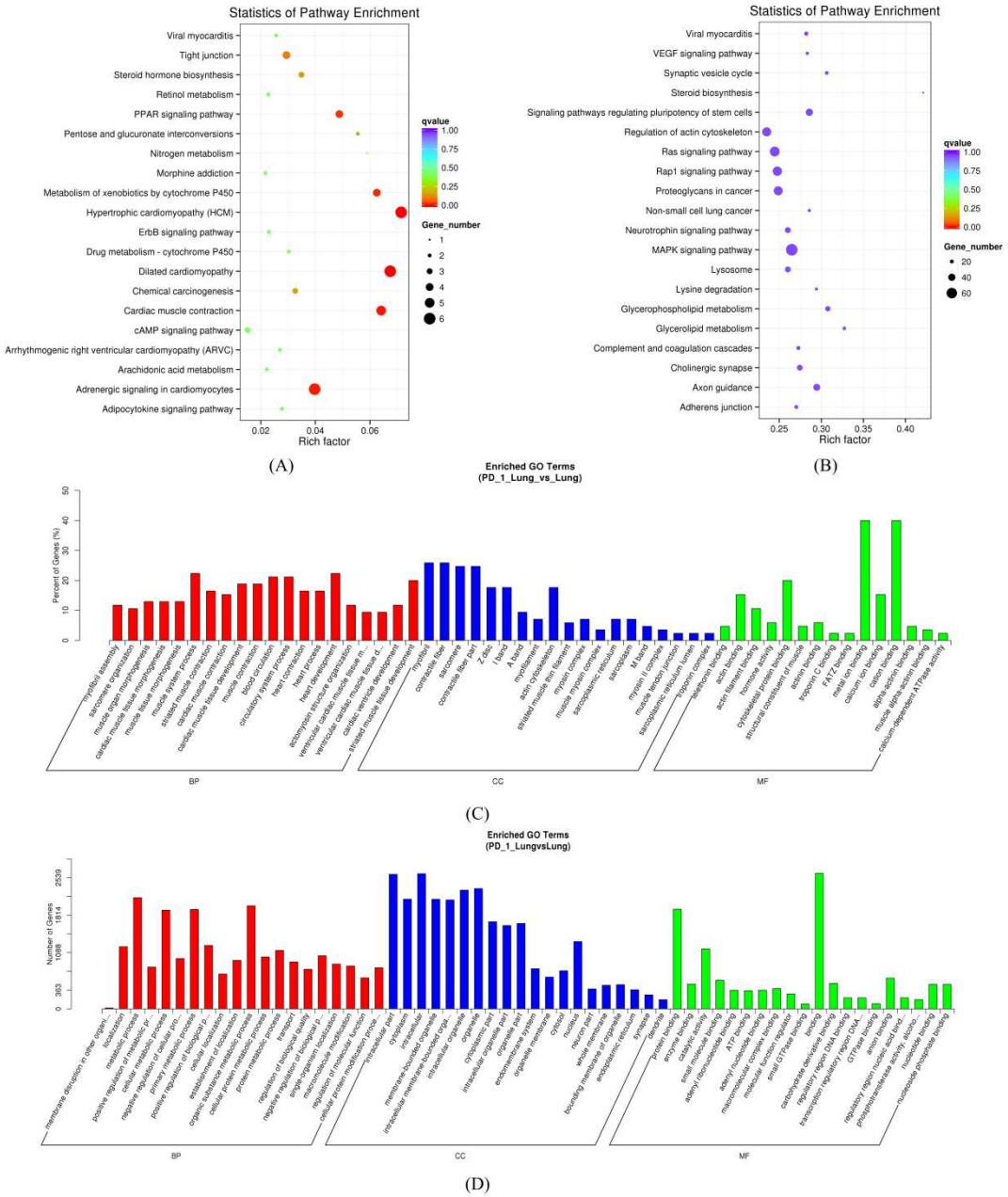

Figure 2. Gene Ontology (GO) and KEGG pathway analysis of dif-mRNAs and dif-miRNAs in the lungs. The top 20 pathways and GO terms (BP (Biological Process), CC (cellular component), and MF (molecular function)) enriched by dif-mRNAs and dif-miRNAs of lungs of the following groups: PD-1 antagonist treatment followed by A/PR8(H1N1) infection group vs. isotype control followed by A/PR8(H1N1) infection group. (A) Top 20 pathways enriched by dif-mRNAs. (B)

Top 20 pathways enriched by dif-miRNAs. (C) Top 20 GO terms enriched by dif-mRNAs. (D) Top 20 GO terms enriched by dif-miRNAs.

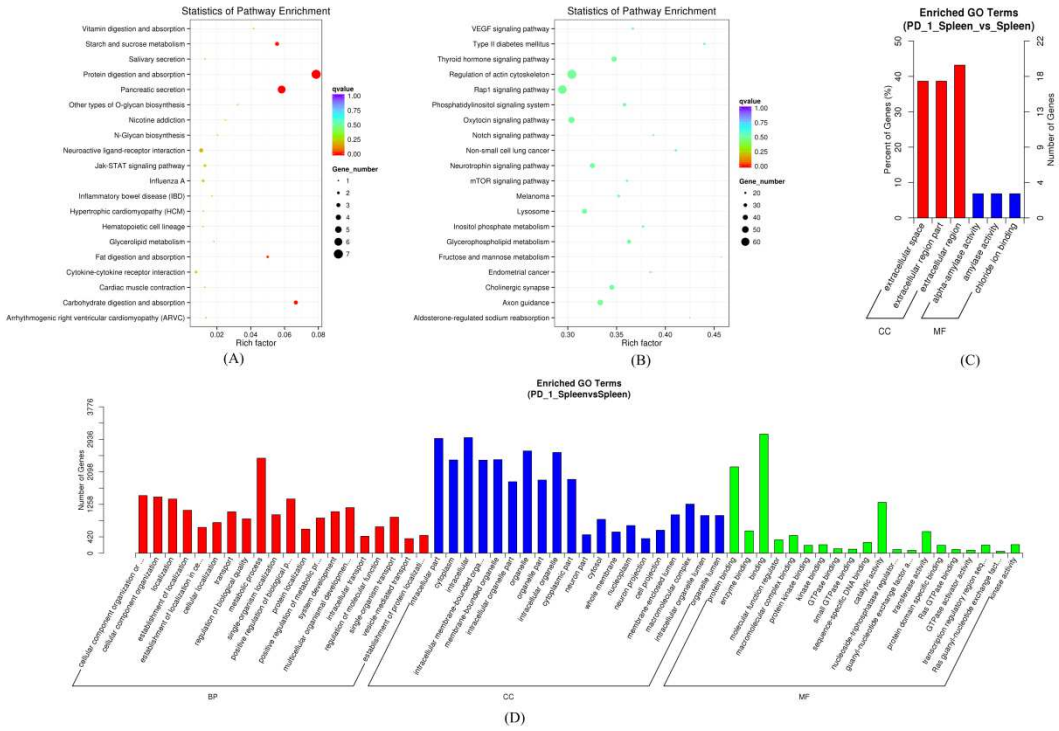

Figure 3. GO and KEGG pathway analysis of dif-mRNAs and dif-miRNAs in spleens.

The top 20 pathways and GO terms (BP (Biological Process), CC (cellular component), and MF (molecular function)) enriched by dif-mRNAs and dif-miRNAs of spleens of the following groups: PD-1 antagonist treatment followed by A/PR8(H1N1) infection group *vs*. isotype control followed by A/PR8(H1N1) infection group. (A) Top 20 pathways enriched by dif-mRNAs (B) Top 20

pathways enriched by dif-miRNAs (C) Top 20 GO terms enriched by dif-mRNAs (D) Top 20 GO terms enriched by dif-miRNAs.

Protein-Protein Interaction (PPI) Network

The PPI network based on dif-mRNAs between lungs consisted of 24 nodes and 24 interaction pairs (Figure 4). Top 10 KEGG pathways enriched by genes in the PPI network were significantly involved in heart damage. The PPI network based on dif-mRNAs between spleens consisted of 10 nodes and 10 interaction pairs (Figure 5).

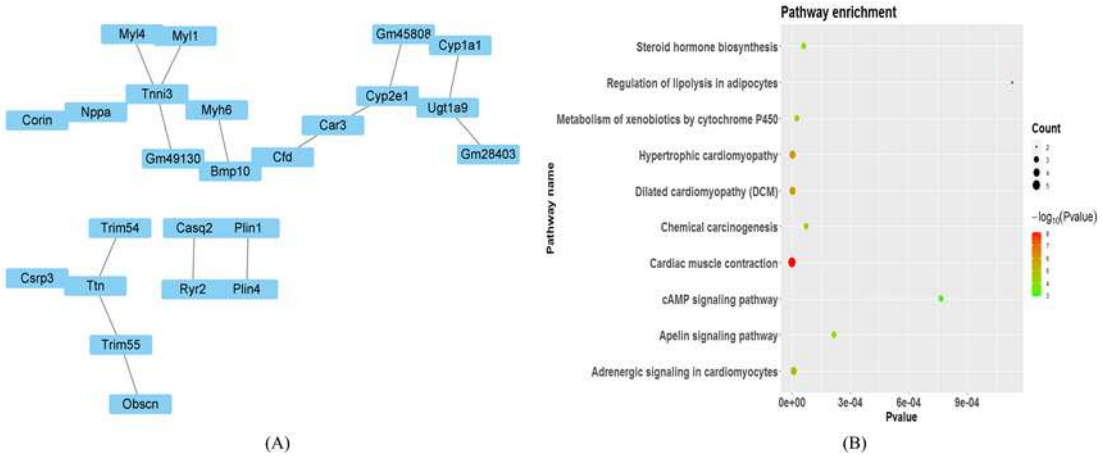

Figure 4. Protein-Protein Interaction (PPI) analysis in the lungs. (A) PPI network of dif-mRNAs in the lungs. (B) Top 10 KEGG pathways enriched by genes in the lung PPI network.

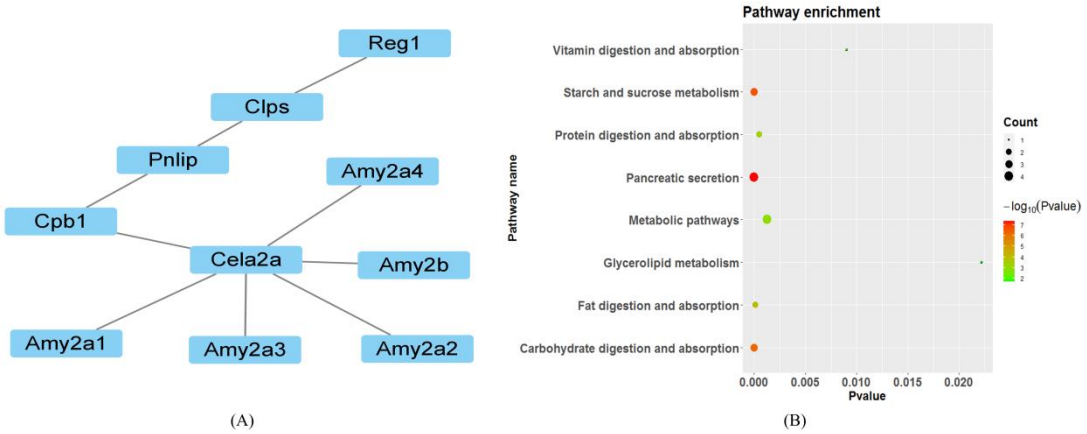

Figure 5. Protein-Protein Interaction (PPI) analysis in the spleens. (A) PPI network of dif-

mRNAs in spleens. (B) Top 8 KEGG pathways enriched by genes in the spleens PPI networks.

Enrichment analysis of lncRNA and circRNA-related target genes

KEGG enrichment and GO analysis was performed for dif-lncRNA and dif-circRNA-related target genes (Figure 6 and Figure 7). The dif- lncRNA target genes were enriched in 100 pathways in lungs and 154 pathways in spleens. The dif- circRNA target genes were enriched in 20 pathways in lungs and 14 pathways in spleens. There was a little degree of overlap of lncRNAs and circRNAs in lungs and spleens between the most enriched clusters except for Hypertrophic cardiomyopathy, MAPK signaling pathway, and the AMP-activated protein kinase (AMPK) signaling pathway.

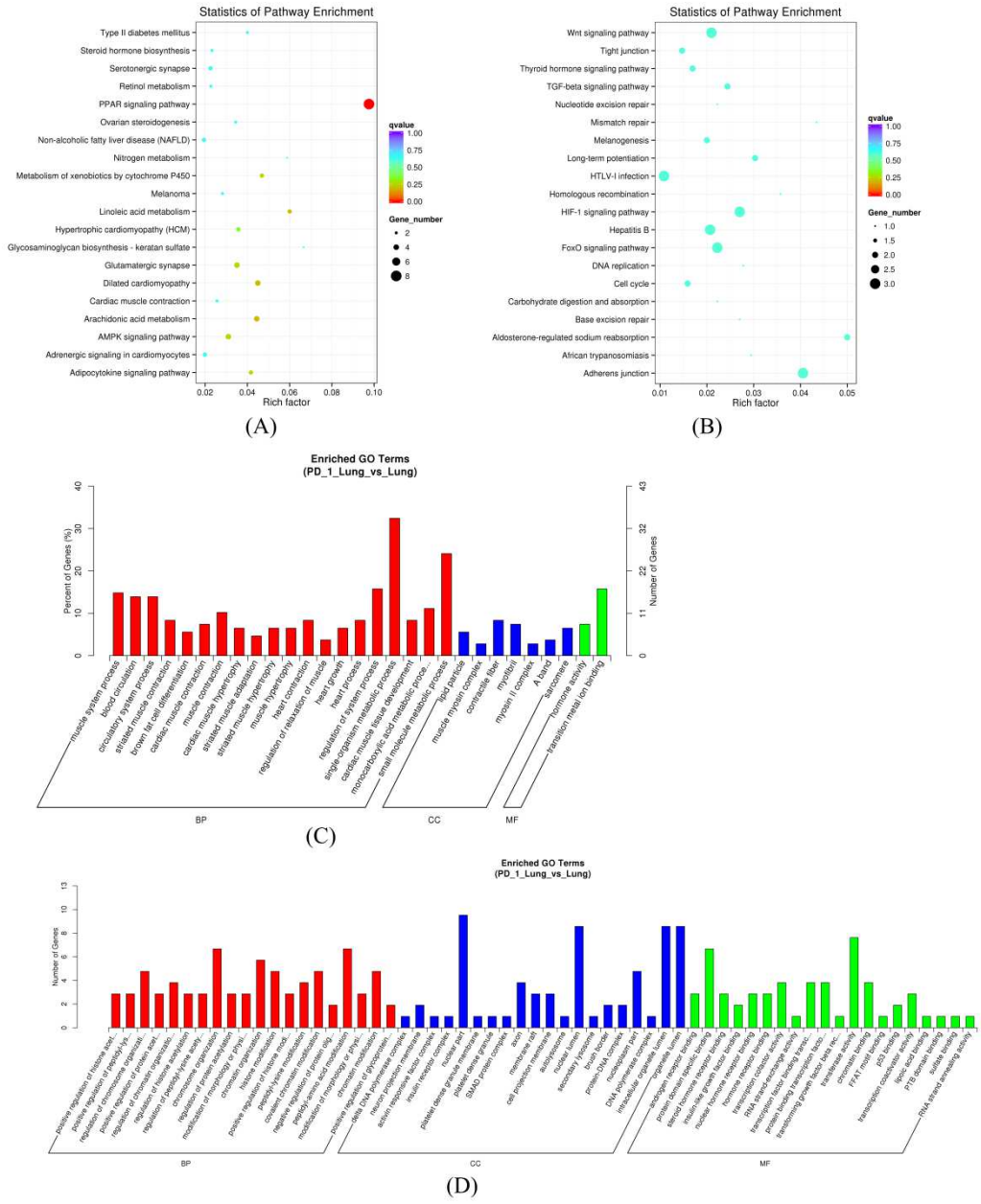

219

220 **Figure 6.** Analysis of GO and KEGG pathways of dif- lncRNAs and dif-circRNAs of the lungs.

221 Top 20 pathways and GO terms (BP (Biological Process), CC (cellular component), and MF

222 (molecular function)) enriched by dif- lncRNAs and dif-circRNAs of the lungs (A) Top 20

223 pathways enriched by dif-lncRNAs. (B) Top 20 pathways enriched by dif-circRNAs (C) Top 20

224 GO terms enriched by dif-lncRNAs (D) Top 20 GO terms enriched by dif-circRNAs.

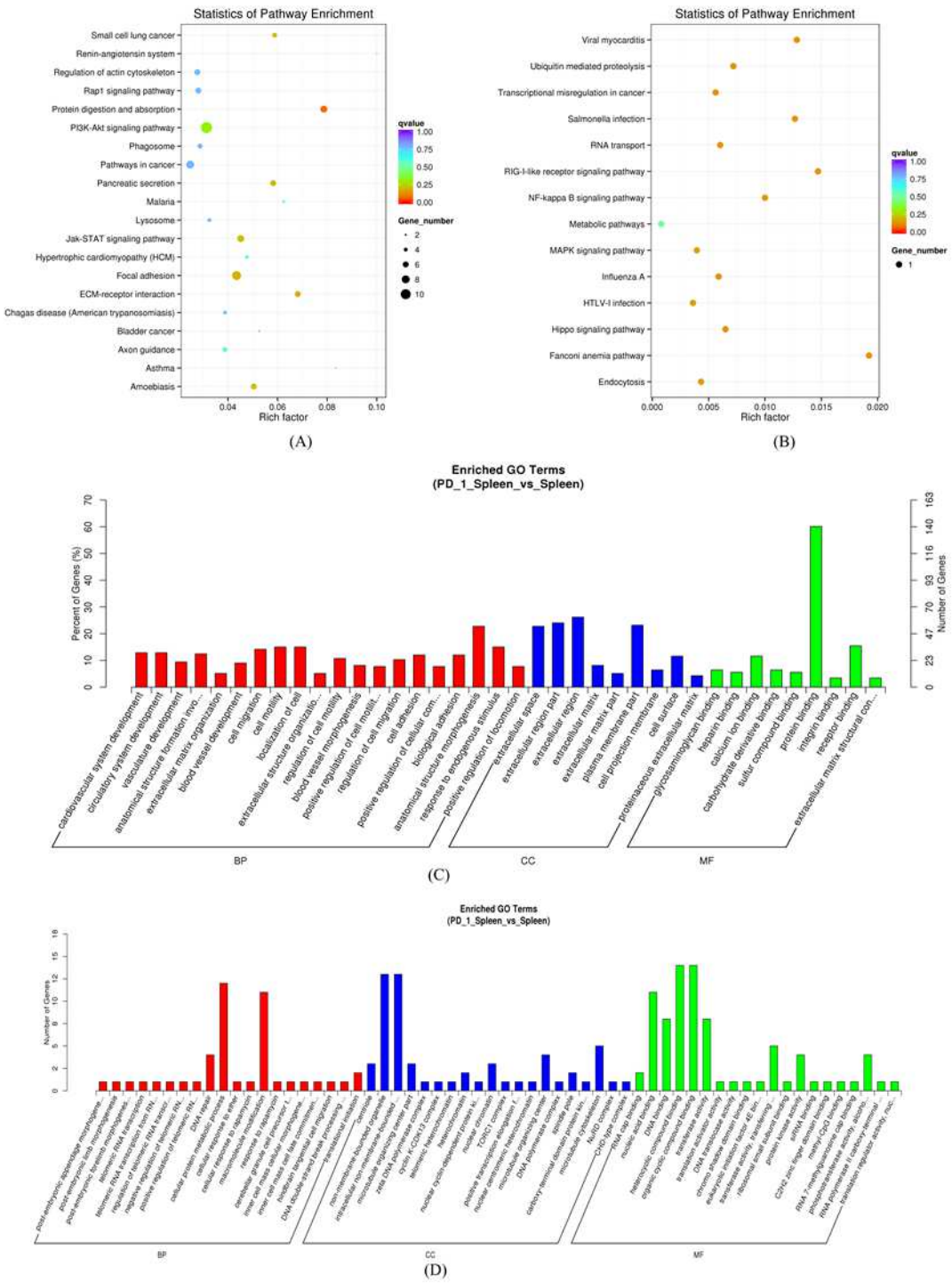

225

226 **Figure 7.** Analysis of GO and KEGG Pathway of dif- lncRNAs and dif-circRNAs of spleens.

227 Top 20 pathways and GO terms (BP (Biological Process), CC (cellular component), and MF

228 (molecular function)) enriched by dif- lncRNAs and dif-circRNAs of spleens (A) Top 20 pathways

229 enriched by dif-lncRNAs. (B) Top 20 pathways enriched by dif-circRNAs. (C) Top 20 GO terms e

nriched by dif-lncRNAs (D) Top 20 GO terms enriched by dif-circRNAs.

Competing Endogenous RNA Network Construction

According to the dif-lncRNA–dif-miRNA pairs and dif-miRNA–dif-mRNA pairs, differentially expressed lncRNAs and mRNAs regulated by the same miRNA were screened. In total, 77 lncRNA-miRNA-mRNA interactions in lungs were finally obtained (Figure 8), including 35 upregulated lncRNAs and 9 downregulated lncRNAs, 5 upregulated and 5 downregulated mRNAs, and 2 upregulated and 5 downregulated miRNAs. In spleens, 131 lncRNA-miRNA-mRNA interactions were finally obtained (Figure 9), including 29 upregulated lncRNAs and 26 downregulated lncRNAs, 17 upregulated and 8 downregulated mRNAs, and 5 upregulated and 4 downregulated miRNAs.

2 interaction relationships of circRNA-miRNA-mRNA in lungs were obtained (Figure 10), comprising 2 upregulated circRNAs, 2 upregulated mRNAs, and one downregulated miRNA. In spleens, 32 interaction relationships of circRNA-miRNA-mRNA were obtained (Figure 11) including 6 upregulated circRNAs and 1 downregulated circRNA, 16 upregulated mRNAs and 2 downregulated mRNAs, 2 upregulated miRNAs and 4 downregulated miRNAs.

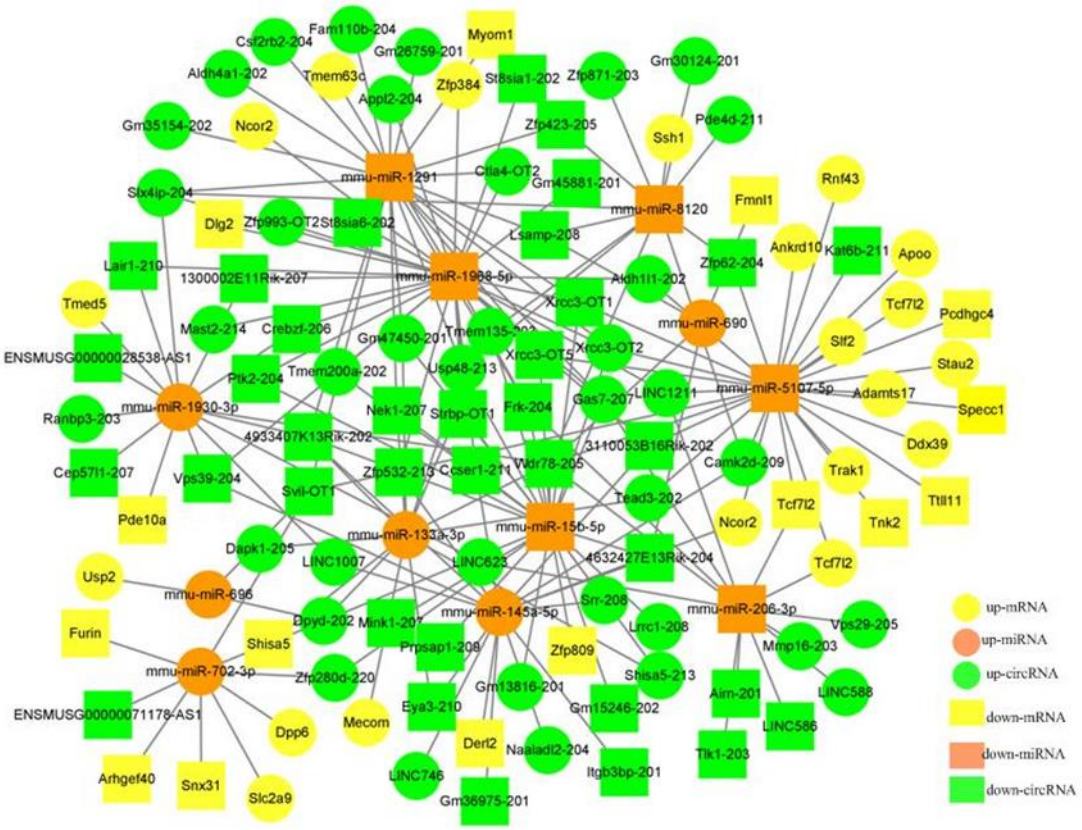

Figure 8. The lncRNA-miRNA-mRNA network of the lungs. Circles represent upregulation and rectangles represent downregulation. mRNAs, miRNAs, and lncRNAs in the network are presented in yellow, orange, and green, respectively.

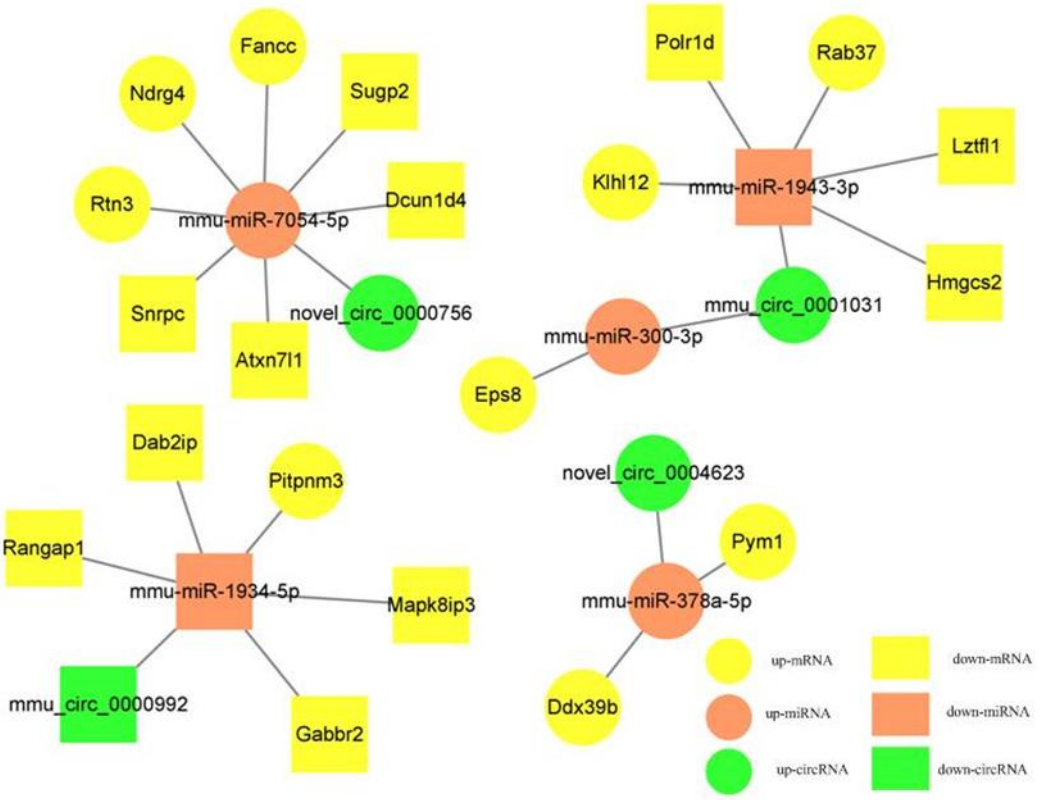

Figure 9. The lncRNA-miRNA-mRNA Network of the spleens. Circles represent upregulation and rectangles represent downregulation. mRNAs, miRNAs, and lncRNAs in the network are presented in yellow, orange, and green, respectively.

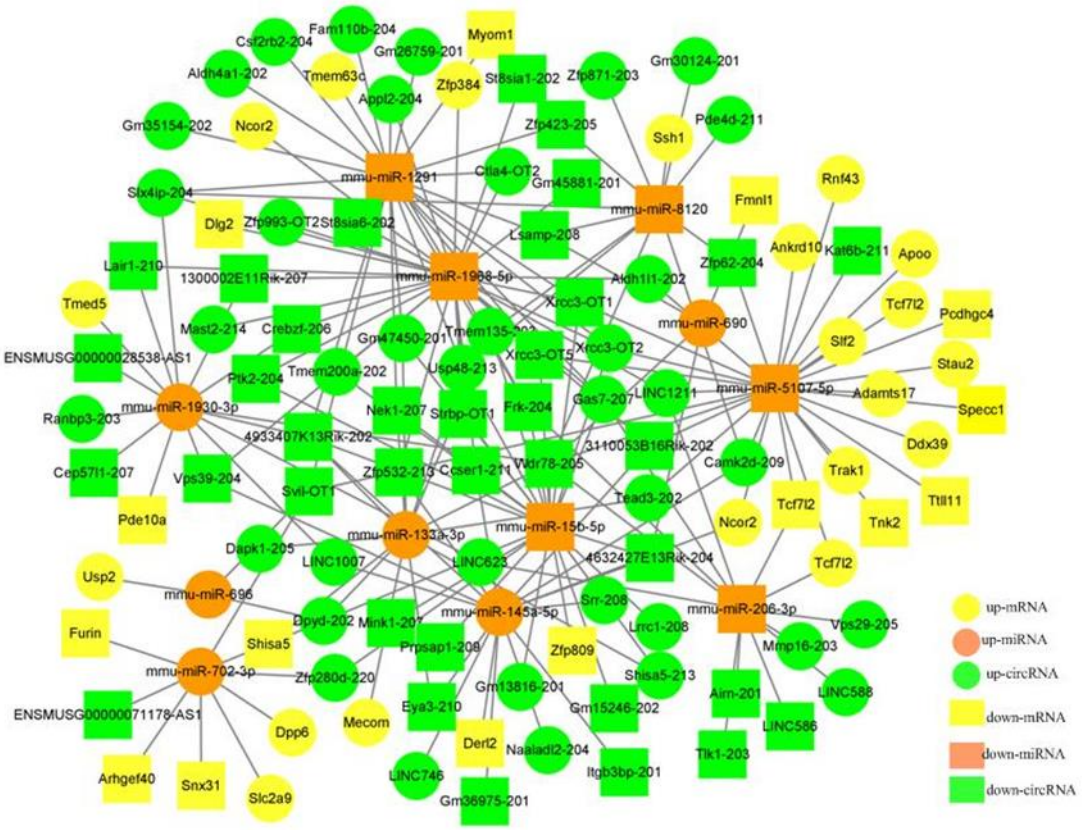

Figure 10. The circRNA-miRNA-mRNA network of the lungs. Circles represent upregulation and rectangles represent downregulation. mRNAs, miRNAs, and circRNAs in the network are presented in yellow, orange, and green, respectively.

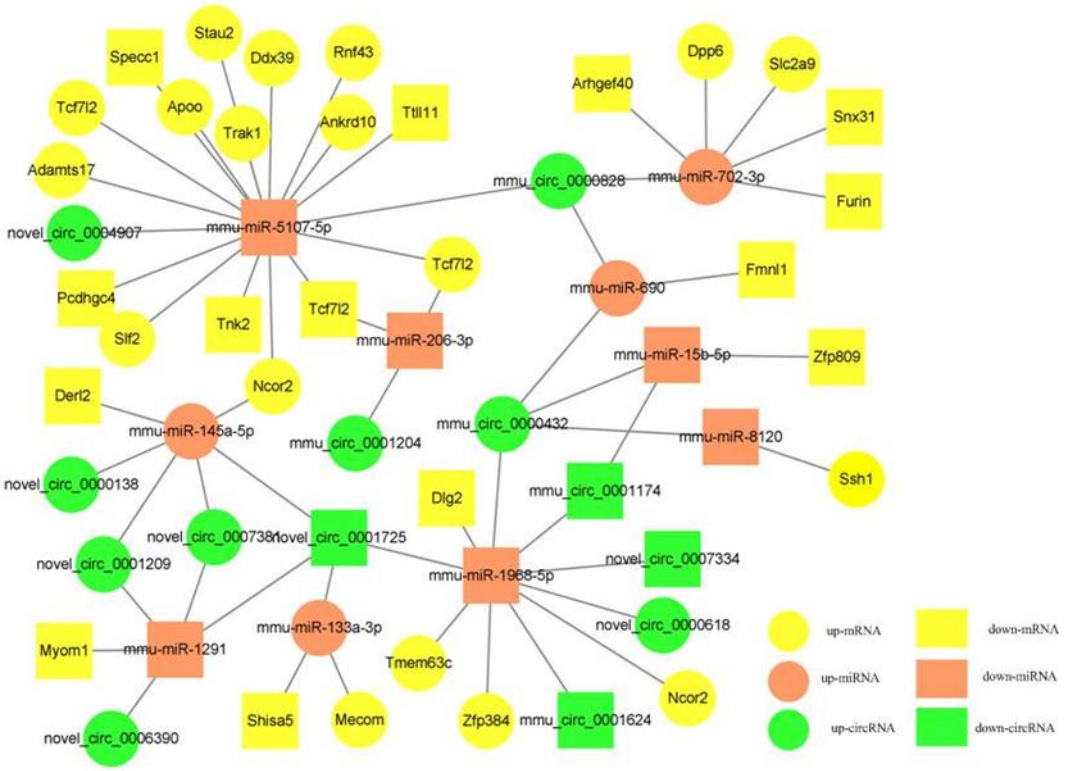

Figure 11. The circRNA-miRNA-mRNA network of the spleens. Circles represent upregulation and rectangles represent downregulation. mRNAs, miRNAs, and circRNAs in the network are presented in yellow, orange, and green, respectively

Further, differentially expressed circRNAs, lncRNAs, and mRNAs that were regulated by the same miRNA were further screened based on the lncRNA-miRNA-mRNA and circRNA-miRNA-mRNA analysis. Finally, 595 interaction pairs were obtained in lungs (Figure 12), comprising 135 upregulated and 63 downregulated mRNAs, 5 upregulated and 5 downregulated miRNAs, 5 upregulated and 2 downregulated circRNAs, and 46 upregulated and 38 downregulated lncRNAs. There were 462 interaction pairs in spleens (Figure 13), comprising 85 upregulated and 64 downregulated mRNAs, 6 upregulated and 6 downregulated miRNAs, 42 upregulated and 36 downregulated circRNAs, and 10 upregulated and 4 downregulated lncRNAs.

Downregulated mmu-miR-7043-3p and Vps39-204 were significantly enriched in the ceRNA network.

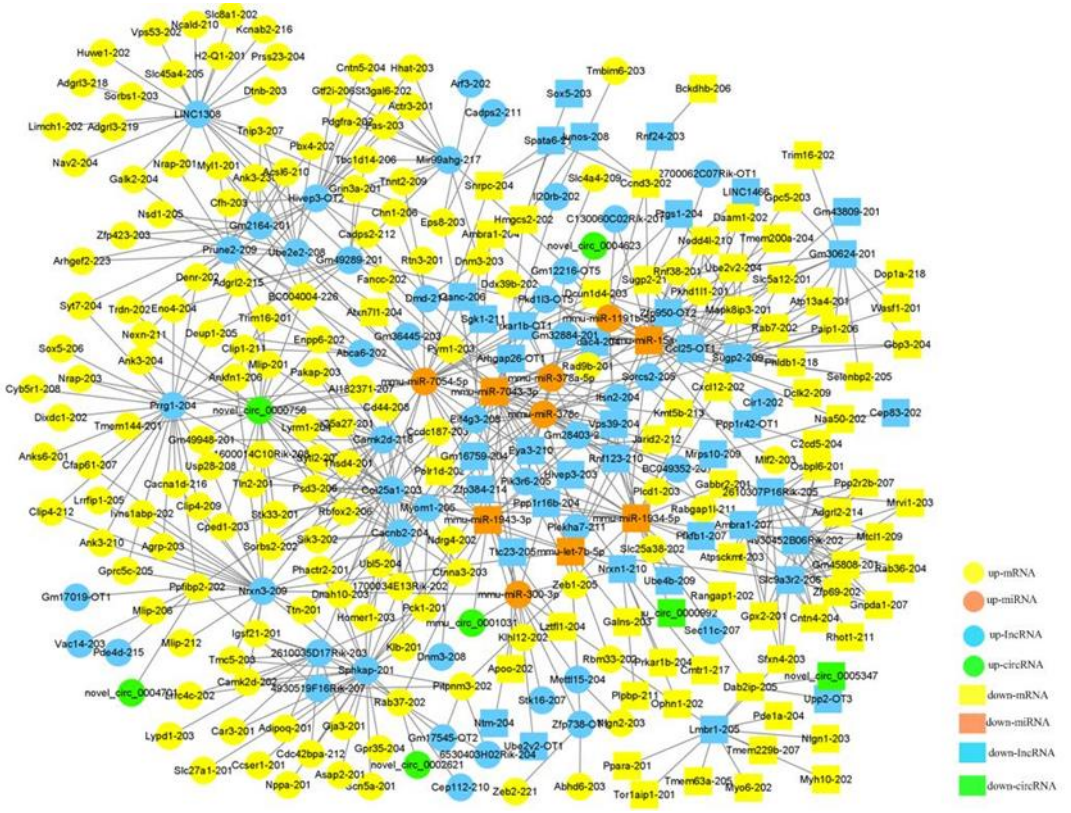

Figure 12. The Competing Endogenous RNA (ceRNA) network of the lungs. Circles represent upregulation and rectangles represent downregulation. mRNAs, miRNAs, lncRNAs, and circRNAs in the network are presented in yellow, orange, blue, and green, respectively.

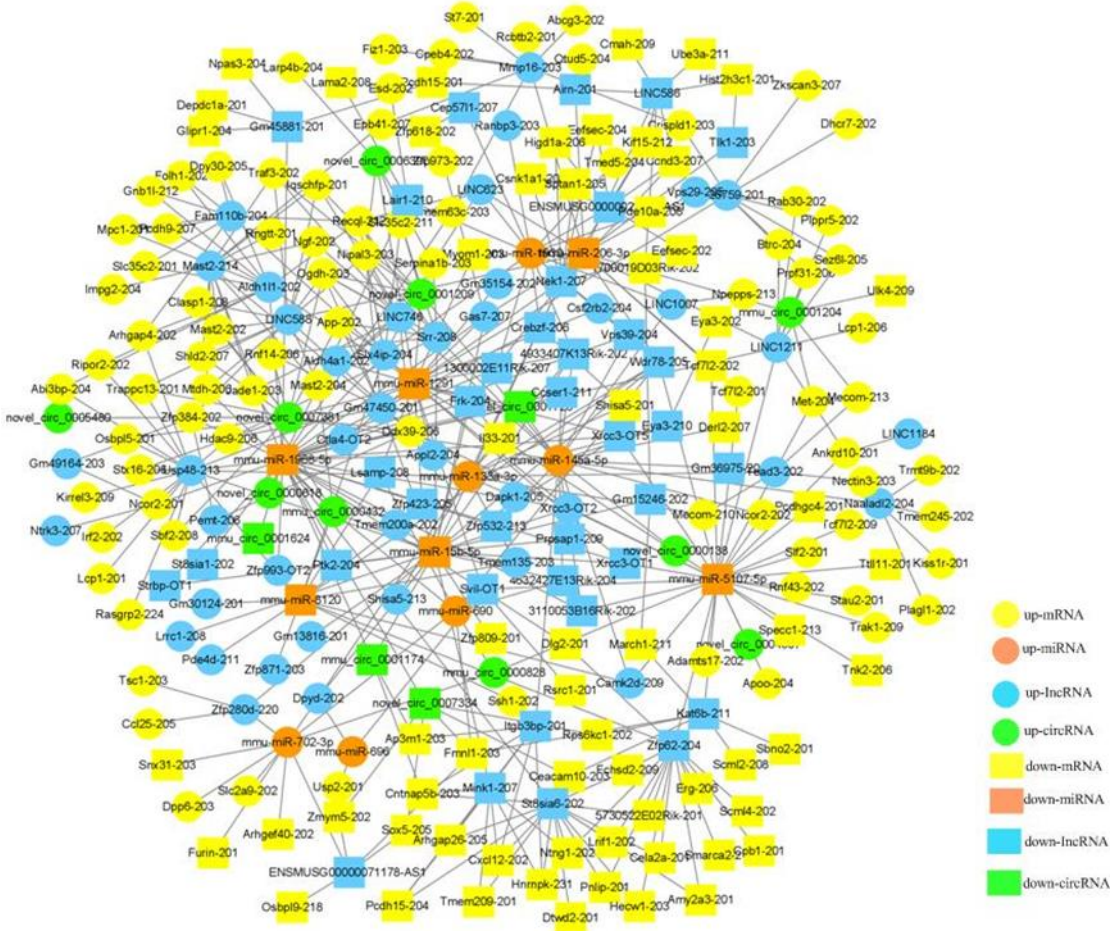

Figure 13. The Competing Endogenous RNA (ceRNA) network of the spleens. Circles represent upregulation and rectangles represent downregulation. mRNAs, miRNAs, lncRNAs, and circRNAs in the network are presented in yellow, orange, blue, and green, respectively.

Discussion

The PD-1/PD-L1 signaling pathway has important regulatory roles in antiviral immune responses, and PD-1/PD-L1 upregulation is induced by persistent viruses, including human immunodeficiency virus (HIV)[13-14], hepatitis C virus (HCV)[15], and hepatitis B virus (HBV)[16], which impairs T cell responses and is unfavorable for virus clearance. Recently, the role of the PD-1/PD-L1 axis during acute virus infection has been further investigated. Upregulated PD-1/PD-L1 expression induced by severe influenza A virus infection is an important component of the immunosuppressive microenvironment, and blocking this signaling pathway will reduce

tissue damage, lower virus titers in the lung, and alleviate symptoms of infection to promote recovery[7-8, 17]. However, the molecular mechanism of the PD-1 checkpoint in the antivirus immune microenvironment are still not well understood and are thus worthy of in-depth investigation.

Next-generation sequencing, which permits massive sequencing with a much higher throughput, has numerous advantages over traditional sequencing technology, and has been applied in various fields of infection disease research, such as identification of infectious pathogens and exploration of the infection mechanism[18-19]. In this study, by applying whole-transcriptome sequencing, we identified 84 dif-mRNAs , 36 dif-miRNAs, 90 dif-lncRNAs, and 22 dif-circRNAs in PD-1 antagonist treated A/PR8(H1N1) influenza infected lungs compared with those in the controls (IgG2a isotype control treated before infection). In the comparison between the spleen samples from the above two groups, 45 dif-mRNAs , 36 dif-miRNAs, 57 dif-lncRNAs, and 24 dif-circRNAs were identified. Direct functional enrichment analysis on the dif-mRNAs and dif-miRNAs showed that these genes were mainly involved in myocardial damage related to viral infection, MAPK signaling pathways, the RAP1 signaling pathway, and Axon guidance.

Functional Enrichment analysis of mRNA and miRNA in lung and spleen clearly highlighted myocardial damage related to viral infection, and PPI analysis was also significantly enriched for viral heart damage. Influenza virus is an etiological agent of myocarditis, and the relationship between acute respiratory virus infection, especially influenza, and associated viral myocardial damage is greatly underestimated. Many studies have reported that influenza virus infection, especially severe infection, causes fatal myocarditis in humans and experimental animals. Acute

cardiovascular events even death triggered by influenza was first noted as early as the 1930s. Several studies have confirmed that acute respiratory infections or influenza-like illnesses were closely related to subsequent acute cardiovascular events[20-21], and autopsies showed that the majority of the heart was affected in fatal cases during epidemics of influenza[22-23]. Viruses might replicate in the heart of at least 10% of patients with infection, and pathological injuries include focal infiltration with inflammatory cells in the interstitial and pericardium areas, myocardial edema, and cardiac necrosis. Frequently, both the left and right sides of heart are dilated[24]. The basic treatment is hemodynamic and ventilatory support; however, the use of immunosuppressive or antiviral therapy for fulminant myocarditis of viral etiology is controversial[25]. Our sequencing result suggested that PD-1 antagonist interferes with virus-induced cardiomyocyte damage and might alleviate tissue damage; however, this conclusion needs to be further confirmed in a larger scale animal experiment.

The MAPK signaling pathway plays an important role in regulating cell proliferation, differentiation, invasion, metastasis, and death through phosphorylation activation. The relationship between MAPK signaling pathways and anti-PD-1 antibody in infectious disease has been discussed elsewhere, especially in chronic infection. MAPK activation is an important initiating event in the upregulation of PD-1 in HIV-1-infected cells, and inhibition of this signaling pathway can reduce infection[26-27]. The HA protein of influenza A virus is conserved among strains and subsets, and axon guidance molecules were proven to have a large pentapeptide overlap, thus immune cross-reactivity between influenza HA and axon guidance molecules is possible[28-30]. PD-1 signaling inhibits Rap guanine nucleotide exchange factor 1 (RAPGEF1 also known as C3G) phosphorylation by utilizing SHP-1/2 (also known as protein tyrosine phosphatase non-receptor

type 6 and type 11), and reduced levels of phosphorylated C3G result in reduced RAP1 activation and adhesion to intercellular adhesion molecule 1 (ICAM-1) to inhibit T-cell adhesion. Several studies suggested that sepsis-induced upregulation of PD-1 has an impact on the motility and migratory capacity of T lymphocytes by regulating classical inhibitory motif recruitment, activation of the phosphatases SHP-1/2, and signaling through RAP1[31].

Additionally, we identified the significant role of downregulated mmu-miR-7043-3p and Vps39-204 in the ceRNA network. Increased expression of mmu-miR-7043-3p was proven to be one of remarkable miRNA signatures of myocardial reductive stress, which is associated with cardiac hypertrophy[32]. Future mechanistic studies are needed to determine the role of miR-7043-3p in PD-1/PD-L1 pathway-associated viral damage in severe influenza infection. VPS39 is a member of the vacuolar tethering complex that promotes late endosome formation, and evidence has shown that silencing VPS39 can increase the proliferation of aged human T cells and memory responses of lysosome-defective T cells in a mouse viral infection model[33], and thus might play important roles in antiviral immunity.

Conclusions

In conclusion, this study explored the molecular mechanism of the PD-1 checkpoint blockade–responsive immune microenvironment during severe influenza infection. Upregulated PD-1/PD-L1 expression-induced by severe IAV infection is an important component of the immunosuppressive microenvironment, and blocking this signaling pathway will regulate the following signal pathways: Myocardial damage related to viral infection, MAPK signaling pathways, Rap1 signaling pathway, and Axon guidance. Downregulated mmu-miR-7043-3p and Vps39-204 were most significantly enriched by PD-1 blockade. However, this study was limited

by a small sample size and limited time points to provide a comprehensive overview of the PD-1 checkpoint blockade–responsive immune microenvironment. Further *in vivo* validation using a larger scale animal experiment and dynamic functional characterization are needed to delineate the exact mechanistic details.

List of abbreviations

The programmed cell death 1: PD-1

PD-1 ligand 1: PD-L1

microRNAs: miRNAs

long noncoding RNAs: lncRNAs

circular RNAs: circRNAs

mitogen activated protein kinase : MAPK)

Ras-related protein 1: RAP1

competing endogenous RNA : ceRNA

dendritic cells : DCs

especially influenza A virus: IAV

acute respiratory distress syndrome : ARDS

gamma interferon: IFN γ

tumor necrosis factor: TNF

RNA sequencing: RNA-Seq

median tissue culture infectious dose: TCID50

phosphate-buffered saline: PBS

small interfering RNAs: siRNAs

PIWI-interacting RNAs: piRNAs

Gene Ontology: GO

Kyoto Encyclopedia of Genes and Genomes: KEGG

weighted gene co-expression network analysis: WGCNA

Biological Process: BP

cellular component: CC

molecular function: MF

Protein-Protein Interaction : PPI

AMP-activated protein kinase : AMPK

human immunodeficiency virus: HIV

hepatitis C virus: HCV

hepatitis B virus: HBV

Rap guanine nucleotide exchange factor 1: RAPGEF1

protein tyrosine phosphatase non-receptor type 6 and type 11: SHP-1/2

intercellular adhesion molecule 1: ICAM-1

Consent to publication

Not applicable

Conflicts of Interest

The authors declare that they have no competing interests

Funding

This work was supported by the Zhejiang Provincial Natural Science Foundation [grant number LQ20H190001].

Ethics

All animal studies were performed in accordance with the Guide for the Care and Use of Laboratory Animals of Zhejiang Province and were approved by the local Ethics Committee.

Availability of data and material:

The datasets used or analyzed during the current study are available from the corresponding author on reasonable request.

Authors' Contributions

HO performed the experiments, analyzed the data, and wrote the first draft. KC and HW reviewed the data and revised the paper. HY designed the experiment and reviewed the data. All Authors read and approved the final version of the article.

Acknowledgements

The Authors would like to thank Elixigen (http://med2708.yixie8.com/) for their assistance with English language editing.

References

1. Ayala, A.; Elphick, G. F.; Kim, Y. S.; Huang, X.; Carreira-Rosario, A.; Santos, S. C.; Shubin, N. J.; Chen, Y.; Reichner, J.; Chung, C.-S., Sepsis-induced potentiation of peritoneal macrophage migration is mitigated by programmed cell death receptor-1 gene deficiency. *Journal of innate immunity* **2014,** *6* (3), 325-338.

2. Han, Y.; Liu, D.; Li, L., PD-1/PD-L1 pathway: current researches in cancer. *American journal of cancer research* **2020,** *10* (3), 727.

3. Topalian, S. L.; Hodi, F. S.; Brahmer, J. R.; Gettinger, S. N.; Smith, D. C.; McDermott, D. F.; Powderly, J. D.; Carvajal, R. D.; Sosman, J. A.; Atkins, M. B.,

421 Safety, activity, and immune correlates of anti¨CPD-1 antibody in cancer. *New*
422 *England Journal of Medicine* **2012,** *366* (26), 2443-2454.
423 4. Sch?nrich, G. n.; Raftery, M. J., The PD-1/PD-L1 axis and virus infections: a
424 delicate balance. *Frontiers in cellular and infection microbiology* **2019,** *9*, 207.
425 5. David, P.; Megger, D. A.; Kaiser, T.; Werner, T.; Liu, J.; Chen, L.; Sitek, B.;
426 Dittmer, U.; Zelinskyy, G., The PD-1/PD-L1 pathway affects the expansion and
427 function of cytotoxic $CD8^+$ T cells during an acute retroviral infection. *Frontiers in*
428 *immunology* **2019,** *10*, 54.
429 6. Palese, P., Influenza: old and new threats. *Nature medicine* **2004,** *10* (12),
430 S82-S87.
431 7. Pauken, K. E.; Godec, J.; Odorizzi, P. M.; Brown, K. E.; Yates, K. B.; Ngiow, S.
432 F.; Burke, K. P.; Maleri, S.; Grande, S. M.; Francisco, L. M., The PD-1 pathway
433 regulates development and function of memory $CD8^+$ T cells following respiratory
434 viral infection. *Cell reports* **2020,** *31* (13), 107827.
435 8. Li, Y. H.; Hu, C. Y.; Cheng, L. F.; Wu, X. X.; Weng, T. H.; Wu, N. P.; Yao, H. P.;
436 Li, L. J., Highly pathogenic H7N9 avian influenza virus infection associated with
437 up-regulation of PD-1/PD-Ls pathway-related molecules. *International*
438 *immunopharmacology* **2020,** *85*, 106558.
439 9. McNally, B.; Ye, F.; Willette, M.; Fla?o, E., Local blockade of epithelial PDL-1 in
440 the airways enhances T cell function and viral clearance during influenza virus
441 infection. *Journal of virology* **2013,** *87* (23), 12916-12924.
442 10. Liang, S. C.; Latchman, Y. E.; Buhlmann, J. E.; Tomczak, M. F.; Horwitz, B. H.;

443 Freeman, G. J.; Sharpe, A. H., Regulation of PD-1, PD-L1, and PD-L2 expression
444 during normal and autoimmune responses. *European journal of immunology* **2003,** *33*
445 (10), 2706-2716.
446 11. Hrdlickova, R.; Toloue, M.; Tian, B., RNA-Seq methods for transcriptome
447 analysis. *Wiley Interdisciplinary Reviews: RNA* **2017,** *8* (1), e1364.
448 12. Nagalakshmi, U.; Waern, K.; Snyder, M., RNA-Seq: a method for comprehensive
449 transcriptome analysis. *Current protocols in molecular biology* **2010,** *89* (1), 4.11.
450 1-4.11. 13.
451 13. Bowers, N. L.; Helton, E. S.; Huijbregts, R. P.; Goepfert, P. A.; Heath, S. L.; Hel,
452 Z., Immune suppression by neutrophils in HIV-1 infection: role of PD-L1/PD-1
453 pathway. *PLoS pathogens* **2014,** *10* (3), e1003993.
454 14. Day, C. L.; Kaufmann, D. E.; Kiepiela, P.; Brown, J. A.; Moodley, E. S.; Reddy,
455 S.; Mackey, E. W.; Miller, J. D.; Leslie, A. J.; DePierres, C., PD-1 expression on
456 HIV-specific T cells is associated with T-cell exhaustion and disease progression.
457 *Nature* **2006,** *443* (7109), 350-354.
458 15. Nakamoto, N.; Kaplan, D. E.; Coleclough, J.; Li, Y.; Valiga, M. E.; Kaminski, M.;
459 Shaked, A.; Olthoff, K.; Gostick, E.; Price, D. A., Functional restoration of
460 HCV-specific $CD8^+$ T cells by PD-1 blockade is defined by PD-1 expression and
461 compartmentalization. *Gastroenterology* **2008,** *134* (7), 1927-1937. e2.
462 16. Peng, G.; Li, S.; Wu, W.; Tan, X.; Chen, Y.; Chen, Z., PD-1 upregulation is
463 associated with HBV-specific T cell dysfunction in chronic hepatitis B patients.
464 *Molecular immunology* **2008,** *45* (4), 963-970.

17. Rutigliano, J. A.; Sharma, S.; Morris, M. Y.; Oguin III, T. H.; McClaren, J. L.; Doherty, P. C.; Thomas, P. G., Highly pathological influenza A virus infection is associated with augmented expression of PD-1 by functionally compromised virus-specific $CD8^+$ T cells. *Journal of virology* **2014,** *88* (3), 1636-1651.

18. Deurenberg, R. H.; Bathoorn, E.; Chlebowicz, M. A.; Couto, N.; Ferdous, M.; Garc¨a-Cobos, S.; Kooistra-Smid, A. M.; Raangs, E. C.; Rosema, S.; Veloo, A. C., Application of next generation sequencing in clinical microbiology and infection prevention. *Journal of biotechnology* **2017,** *243*, 16-24.

19. Mutz, K.-O.; Heilkenbrinker, A.; L?nne, M.; Walter, J.-G.; Stahl, F., Transcriptome analysis using next-generation sequencing. *Current opinion in biotechnology* **2013,** *24* (1), 22-30.

20. Mamas, M. A.; Fraser, D.; Neyses, L., Cardiovascular manifestations associated with influenza virus infection. *International journal of cardiology* **2008,** *130* (3), 304-309.

21. Ukimura, A.; Satomi, H.; Ooi, Y.; Kanzaki, Y., Myocarditis associated with influenza A H1N1pdm2009. *Influenza research and treatment* **2012,** *2012*.

22. Collins, S. D., Excess mortality from causes other than influenza and pneumonia during influenza epidemics. *Public Health Reports (1896-1970)* **1932**, 2159-2179.

23. Kodama, M., Influenza myocarditis. *Circulation Journal* **2010,** *74* (10), 2060-2061.

24. Gupta, S.; Markham, D. W.; Drazner, M. H.; Mammen, P. P., Fulminant myocarditis. *Nature clinical practice cardiovascular medicine* **2008,** *5* (11), 693-706.

487 25. Ammirati, E.; Veronese, G.; Cipriani, M.; Moroni, F.; Garascia, A.; Brambatti, M.;
488 Adler, E. D.; Frigerio, M., Acute and fulminant myocarditis: a pragmatic clinical
489 approach to diagnosis and treatment. *Current cardiology reports* **2018,** *20* (11), 1-12.
490 26. Muthumani, K.; Choo, A. Y.; Shedlock, D. J.; Laddy, D. J.; Sundaram, S. G.;
491 Hirao, L.; Wu, L.; Thieu, K. P.; Chung, C. W.; Lankaram, K. M., HIV-1 Nef induces
492 Programmed Death (PD)-1 expression through a p38 MAPK dependent mechanism.
493 *Journal of virology* **2008**.
494 27. Muthumani, K.; Choo, A. Y.; Shedlock, D. J.; Laddy, D. J.; Sundaram, S. G.;
495 Hirao, L.; Wu, L.; Thieu, K. P.; Chung, C. W.; Lankaraman, K. M., Human
496 immunodeficiency virus type 1 Nef induces programmed death 1 expression through a
497 p38 mitogen-activated protein kinase-dependent mechanism. *Journal of virology* **2008,**
498 *82* (23), 11536-11544.
499 28. Lu, L. Y.; Askonas, B. A., Cross-reactivity for different type A influenza viruses
500 of a cloned T-killer cell line. *Nature* **1980,** *288* (5787), 164-165.
501 29. Lucchese, G.; Capone, G.; Kanduc, D., Peptide sharing between influenza A
502 H1N1 hemagglutinin and human axon guidance proteins. *Schizophrenia bulletin* **2014,**
503 *40* (2), 362-375.
504 30. Wiwanitkit, S.; Wiwanitkit, V., Influenza A H1N1 hemagglutinin and human axon
505 guidance proteins: Peptide sharing but not same epitopes. *Indian journal of human*
506 *genetics* **2013,** *19* (4), 512.
507 31. Azoulay-Alfaguter, I.; Strazza, M.; Pedoeem, A.; Mor, A., The coreceptor
508 programmed death 1 inhibits T-cell adhesion by regulating Rap1. *Journal of Allergy*

509 *and Clinical Immunology* **2015,** *135* (2), 564-567. e1.

510 32. Quiles, J. M.; Narasimhan, M.; Shanmugam, G.; Mosbruger, T.; Rajasekaran, N.

511 S., A novel microRNA signature in myocardial reductive stress. *Free Radical Biology*

512 *and Medicine* **2016,** *100*, S149.

513 33. Olingy, C., Rewiring aged T cells. American Association for the Advancement of

514 Science: 2021.

515